Formation of Polymer-like Nanochains with Short Lithium–Lithium Distances in a Water-in-Salt Electrolyte

Kateryna Goloviznina, Alessandra Serva, Mathieu Salanne

Formation of Polymer-Like Nanochains with Short Lithium-Lithium Distances in a Water-in-Salt Electrolyte

Kateryna Goloviznina,[1,2] Alessandra Serva,[1,2] and Mathieu Salanne[1,2,3,a)]
[1)] *Sorbonne Université, CNRS, Physicochimie des Électrolytes et Nanosystèmes Interfaciaux, F-75005 Paris, France*
[2)] *Réseau sur le Stockage Electrochimique de l'Energie (RS2E), FR CNRS 3459, 80039 Amiens Cedex, France*
[3)] *Institut Universitaire de France (IUF), 75231 Paris, France*

Water-in-salts (WiS) have recently emerged as promising electrolytes for energy storage applications, ranging from aqueous batteries to supercapacitors. Here, *ab initio* molecular dynamics is used to study the structure of a 21 m LiTFSI WiS. The simulation reveals a new feature, in which the lithium ions form polymer-like nanochains that involve up to 10 ions. Despite the strong Coulombic interaction between them, the ions in the chains are found at a short distance of 2.5 Å. They display a drastically different solvation shell compared to the isolated ions, in which they share on average two water molecules. The nanochains have a highly transient character due to the low free energy barrier for forming/breaking them. Providing new insights into the nanostructure of WiS electrolytes, our work calls for re-evaluating our current knowledge of highly concentrated electrolytes and the impact of the modification of solvation of active species on their electrochemical performances.

I. INTRODUCTION

Water-in-salts (WiS), solutions in which the salt outnumbers the solvent in terms of volume and weight, are among the liquid electrolytes receiving most attention in the last years for electrochemical energy storage.[1,2] The first WiS, an aqueous solution of lithium bis-(trifluoromethyl)sulfonylimide (LiTFSI) with a molality of 21 m, was reported to expand the electrochemical stability window of water up to nearly 3V,[3] spurring a rebirth of research on aqueous batteries. Since then, numerous experimental and theoretical studies have been devoted to characterize the physico-chemical properties of WiS, revealing peculiar characteristics compared to conventional electrolytes. Combining various spectroscopies (Raman, infrared, nuclear magnetic resonance) with classical molecular dynamics (CMD) simulations, it was shown that almost all of the water molecules are coordinated to the Li cations, forming relatively long-lived $Li(H_2O)_n^+$ clusters, which promote Li diffusion and lead to high conductivity of the liquid.[4] This organization at short-range leads to the disruption of the usual water hydrogen bond network, with only a few free water molecules. Nano-heterogeneities with characteristic lengths of 1 to 2 nm were further highlighted by small-angle neutron scattering and CMD simulations.[5] The anions tend to self-aggregate in nanodomains, with cations-water clusters forming a 3D percolating network. The structural organization found in the bulk electrolyte alters the properties of the electrode/electrolyte interface,[6] mitigating hydrogen evolution reaction and degradation reactions and resulting in improved electrochemical performances of WiS.[7,8]

Despite the agreement between previous studies on the existence of $Li(H_2O)_n^+$ clusters, the various structures provided by CMD simulations[5,7] display significant discrepancies, in particular for the typical Li-Li distances (Fig. S1) and the Li-O coordination numbers (Fig. S2). It is well known that the results depend on the choice of the force field, and in particular depending on the handling of polarization interactions.[5,9–17] A way to circumvent this problem is to use more accurate *ab initio* MD (AIMD)[18–21] and/or machine-learning based MD.[22] For example, AIMD was used to probe the formation of complex 3D structures in localized high-concentration electrolytes.[18,19] However no lithium chains were evidenced in this study, probably due to the use of other solvents than water. Two studies focused on the calculation of spectroscopic features[20] and the reactivity[22] of the LiTFSI WiS, but the nanostructure of the system was not analyzed in details.

In this work, we employ AIMD at the Density Functional Theory level to investigate a 21 m LiTFSI WiS. By simulating a large system made of 128 ion pairs and 340 water molecules for 70 ps, we show that Li^+ cations associate within the aqueous nanodomains to form polymer-like nanochains inside the liquid. The chains have a strongly transient nature, which can be understood based on very low free energy barriers to switch to and from the isolated ions. Finally, the microscopic solvation mechanism at play is analyzed in detail, and comparison with the recent literature shows that such structures may be more frequent than initially thought.

II. RESULTS AND DISCUSSION

When studying conventional lithium ion-based electrolytes at the molecular level, the focus is often put on the first solvation shell of lithium cations, and how it is shared between water molecules and anions. How-

[a)] Electronic mail: mathieu.salanne@sorbonne-universite.fr

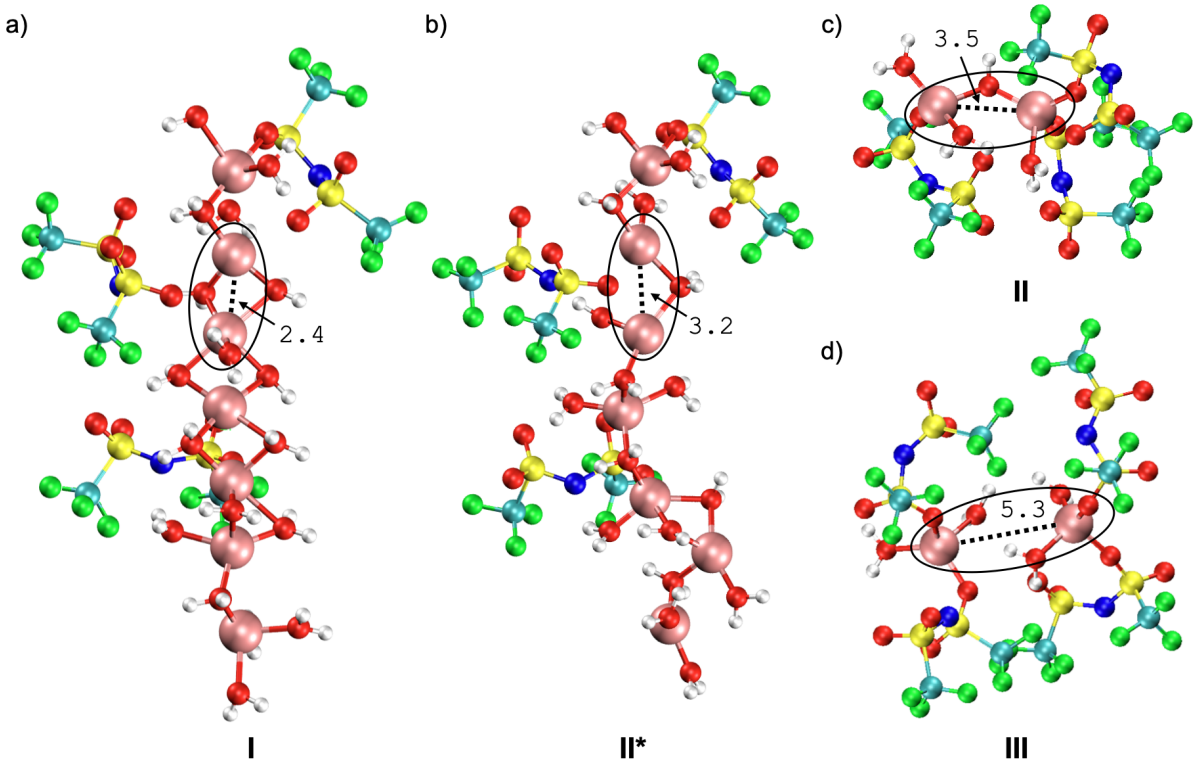

FIG. 1. Local structure of lithium ions in three solvation environments: I (a), II (b,c), III (d). The subfigures (a) and (b) correspond to the linear and disrupted nanochain, and the subfigures (c) and (d) to a pair of lithium ions at larger separation. Red-pink solid lines correspond to the $Li^+ \cdots O$ non-bonded interactions at separations smaller than 2.8 Å.

ever, a global look at the nanoscale structure is necessary for highly concentrated systems.[23] In the case of the LiTFSI WiS, the formation of two 3D percolating networks was evidenced.[5,15] For this reason, it is necessary to perform simulations on a system with large dimensions compared to conventional AIMD studies of aqueous electrolytes, which are usually restricted to one or a few ion pairs and typically ≈100 water molecules. The structure factor obtained by small-angle neutron scattering for the LiTFSI WiS is characterized by a peak around 0.45 to 0.50 $Å^{-1}$,[5] which is representative of nanostructures of size ≈ 1.4 nm, so that a simulation cell of dimension 3.464 nm was used in the present study, that contains 128 ion pairs and 340 water molecules. In addition, the timescales associated to the relaxation of such nanodomains are usually significantly longer than the typical solvation timescales (which are of the order of 1-10 ps), so that long trajectories of 70 ps were gathered.

In agreement with previous works, the formed nanodomains are enriched in water or in anions, respectively, while the Li^+ cations participate in both. Interestingly, the radial distribution functions (RDFs) showed the existence of pairs of lithium ions for some force fields at rather short distances (Figure S1), which was attributed to the aqueous-rich domains.[13,24,25] The most stringent proof was provided for another WiS made of $LiNO_3$.[7] In that case, the combination of x-ray diffraction and MD simulation showed the formation of polymer-like lithium chains, albeit with rather large distance (i.e. larger than 3.5 Å) between neighbour Li^+ ions. In this work, we confirm the latter study, with lithium ions forming nanochains of different sizes inside the liquid after a sufficiently long (70 ps) AIMD simulation. However, as illustrated on Figure 1a), $Li^+ \cdots Li^+$ pairs are observed at distances much smaller than 3.0 Å. These structures are very short-lived: We observe many formation/breaking events during our simulation. The ions are mainly arranged into linear nanochains, with some branches occasionally appearing during the growth process. Several episodes of the linearity spontaneously being disrupted for 2–3 ps are observed during the run, leading to the structure shown on Figure 1b). This results in the fraction of polymerized lithium ions fluctuating in the range of 5–20 %. The absence of such structures in CMD simulations (Figure S3a) points towards the necessity to include electronic structure effects for observing them.

The comparison of the computed structure factor, S(q), to the x-ray (Figure 2d, Figure S4a) and neutron (Figure S4b,c) scattering shows that the simulated liquid structure agrees well with the experimental results. However, previous CMD studies that did not include short lithium-lithium chains (but had a similar medium-range

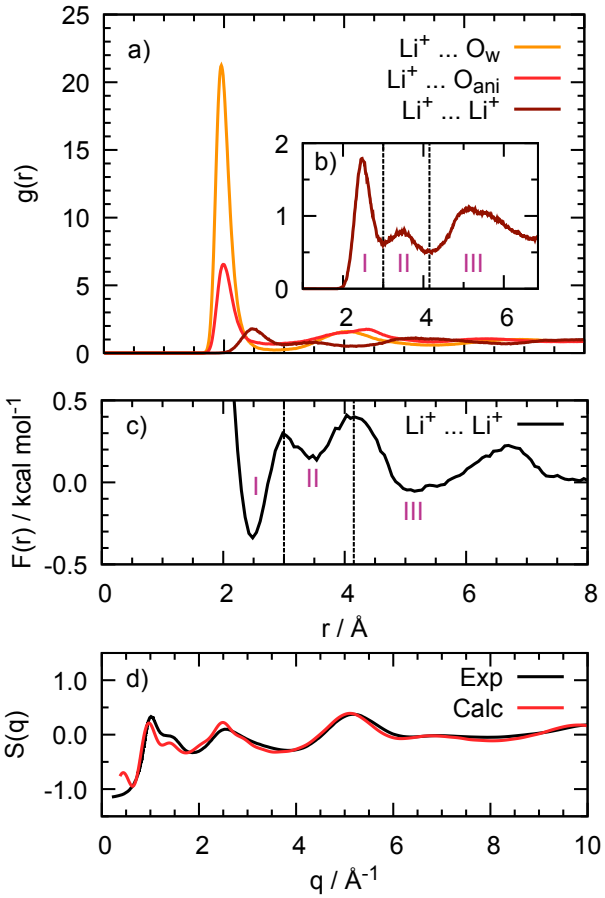

FIG. 2. (a) Radial distribution functions (RDFs, $g(r)$) of the oxygen atoms of the anion (O_{ani}), water (O_w), and lithium ions around the lithium cation. The inset (b) shows a magnified view of the $Li^+\cdots Li^+$ RDF, with the distance definition of three different Li^+ solvation environments. The dashed lines correspond to the first (3.0 Å) and second (4.1 Å) minima of the RDF. (c) The $Li^+\cdots Li^+$ free energy profile as a function of separation between cations obtained from the RDF in panel (b). (d) Structure factor of LiTFSI WiS system computed from the simulation and compared to x-ray scattering experiments.[9]

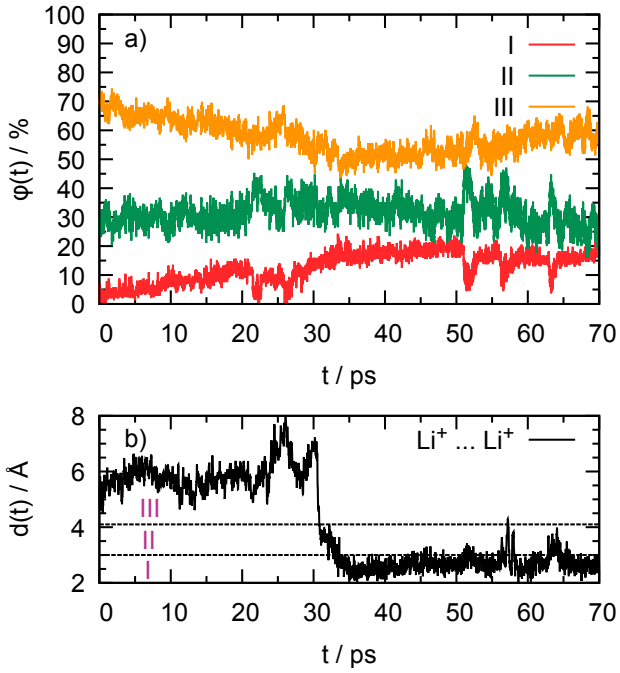

FIG. 3. (a) Time evolution of the fraction of the lithium cations ($\phi(t)$) involved into three solvation environments (I, II, and III). (b) Example of a time evolution of a distance between two lithium cations which undergo a III→II→I transition.

structure as in the current work), also display similar agreement.[10] This is due to the fact that the $Li^+\cdots Li^+$ contribution remains relatively small as illustrated by the partial S(q) in Figure S4d-f. We also note that the structure of the solvation shell of the Li^+ ions is also in good agreement with most of previous CMD studies (Figures S2, S5), showing that the latter generally catch well the solvation effects.

In order to refine the characterization of the nanochains formation, Figure 2a-b displays the Li-O and Li-Li partial RDFs. We observe that the closest $Li^+\cdots Li^+$ contacts are located at about 2.5 Å, being notably shorter than that predicted in the literature by CMD (Figure S1) and within the range of the Li-O first solvation shell. This first peak at 2.5 Å is then followed by two other peaks with lower intensities at 3.5 Å and 5.3 Å. Therefore, three structural environments cohabit for the Li cations. Based on the corresponding minima of the RDF, we note them I for $r \leq 3.0$ Å, II for 3.0 Å $< r \leq$ 4.1 Å and III for $r >$ 4.1 Å - typical snapshots of the various environments are shown on Figures 1 and S3b,c. The lithium nanochains correspond to environment I, and the episodes of its disruption to that of II. However, it should be noted that the fraction of contribution II varies from 20 % to 50 %, being higher than that of I (Figure 3a). This is because not only non-linear lithium chains belong to this environment, but also other polymeric structures (mainly, lithium pairs, Figure S3c), which try to further arrange into chains. Environment III remains the dominant contribution in the solution (45–75 %) and corresponds to isolated solvated lithium cations. The free energy barriers, as estimated from the corresponding $Li^+\cdots Li^+$ potential of mean force, are rather small, not exceeding 0.6 kcal mol^{-1} (Figure 2c), which corresponds to about 1 k_BT, for all the transitions. This means that, due to the thermal fluctuations, lithium solvation can dynamically switch from one environment to another on relatively short timescales. This dynamical exchange is illustrated in Figure 3, which shows that the concentration of the three environments varies along the simulation (panel a), and through the variation of the Li-Li distance during a III→II→I transition (panel b).

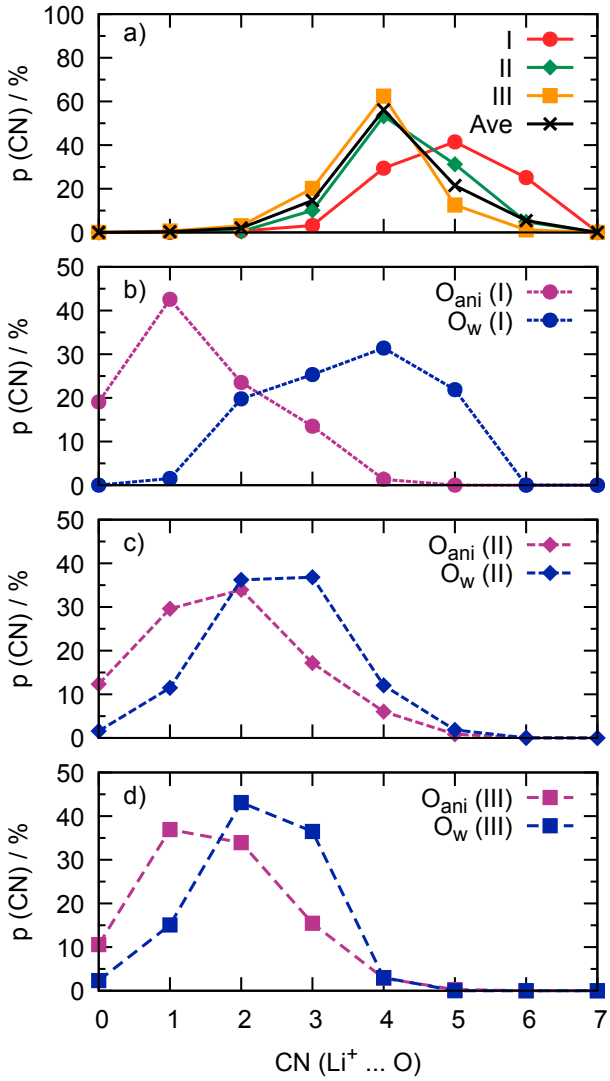

FIG. 4. Probabilities of finding a specific number of O atoms in the first Li^+ coordination shell (a-d). Subfigure (a) considers the total number of O atoms in the first Li^+ solvation shell, while subfigures (b-d) represent O from the $TFSI^-$ anion (O_{ani}) and of water molecules (O_w) separately.

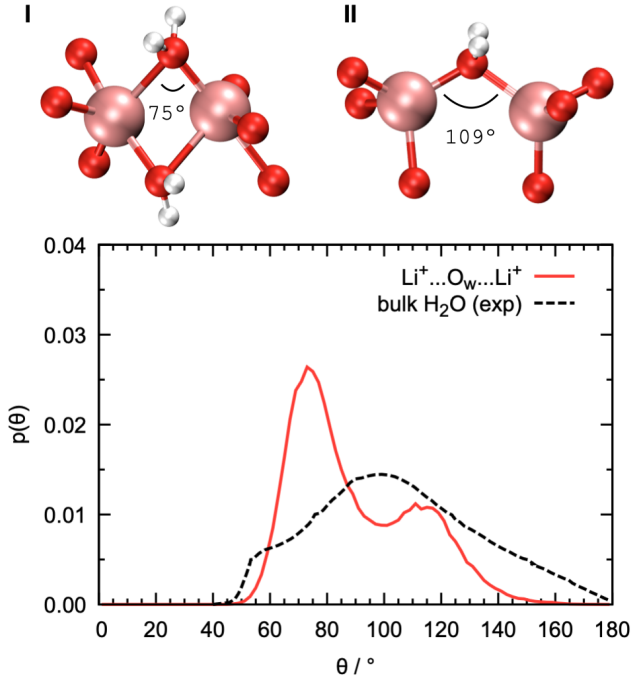

FIG. 5. The $Li^+ \cdots O_w \cdots Li^+$ angle probability distribution with the corresponding snapshots representing the most probable angles in environments I and II. The dashed line refers to the experimental $O_w \cdots O_w \cdots O_w$ angle probability distribution, obtained from joint x-ray and neutron scattering data.[26]

Formation of the lithium nanochains is not favorable unless some solvent molecules and anions can compensate for the local excess of positive charge. The most probable interaction of lithium cations with oxygen atoms of water and of $TFSI^-$ occurs at 1.9–2.0 Å and the first coordination shell extends up to 2.8 Å (Figures 2a, S6). On average (Figure 4a), the most likely total coordination number (CN) of lithium is 4 (56 % of cases) that corresponds to a tetrahedral geometry, although CNs of 3 and 5 are also observed in 15 % and 21 % of cases, respectively. If we now compute the CN for the different lithium environments, we observe that the local environment I is strikingly different from the average representation, as well as from environments II and III. The most probable total coordination numbers are higher, ranging from 4 to 6 (29 %, 42 % and 25 %, respectively). By decomposing the total CN in water and anion contributions, Figure 4b shows that the cation is surrounded by 2–5 water molecules, and often (43 % of cases) one anion is found nearby. Such close lithium contacts are achieved by sharing one - three water molecules (and sometimes one or rarely two anions) as shown in Figures 1a, S7a, S8. The presence of several bringing species enforces the geometry of the lithium nanochains to be linear. This leads to notable deviations from tetrahedral coordination of the involved water molecules: the $Li^+ \cdots O_w \cdots Li^+$ angle attains 65–75° as shown in Figure 5, which remains within the experimentally reported angles between water molecules in the pure liquid.[26] The structure of our nanochains agrees with the previously reported results on highly concentrated $LiNO_3$ solutions. Despite the difficulty in catching the lithium-lithium environment by scattering experiments, the analysis made in Ref. 7 concluded that the typical distances between some water molecules are explained by the formation of bridged structures between lithium ions similar to the ones shown on Figure 1, with a general formula $(Li(H_2O)_2)_n$.

Moving to environment III, we can see that the probability distribution of the total CN is very similar to the average picture. The dominant total value is 4, result-

ing in 2 + 2 or 3 + 1 water and anion species in the first solvation shell of lithium (Figure 4d). The geometry of such a complex is close to a tetrahedra as depicted in Figure 1d. Surprisingly, the probability of finding a cation in a completely symmetrical environment, solvated solely by water molecules, is rather low (about 3 %). Finally, the CN distributions of environment II (Figure 4a,c) are quite similar to those of III. Nonetheless, the tetrahedral geometry of lithium coordination shells becomes partially distorted when approaching each other, i.e corresponding to the transition III→II. Attempting to reach closer contact, lithium cations start sharing one water molecule (Figure 1c,S7b), and the Li···Ow···Li angle reaches 110–115° (Figure 5), which corresponds to an almost perfectly tetrahedral environment. Further II→I transition becomes possible only in the presence of a second shared water (or an anion) since one "bridging" molecule is not sufficient to stabilize a lithium-lithium dimer formation.

As mentioned before, a second minor contribution to environment II comes from the distortion of nanochains into non-linear chains (Figure 1b, denoted as II*). This is reflected in a more notable contribution of CN = 5 compared to environment III, associated with greater fractions of $CN_w = 3$ and $CN_{ani} = 2$ as shown in Figure 4c. The I→II transition starts from the loss of one bridging species, due to which two neighboring lithium ions are repelled from each other by about an extra 1 Å. It causes breaking down the linearity of the chain, and cations are found in an irregular solvation environment, intending to arrange back into the nanochains. Therefore, environment II should be interpreted as a metastable state between environments I and III, with low energy barriers ($< 0.25\,\mathrm{kcal\,mol^{-1}}$) towards both directions (Figure 2c).

Such a close approach of metal aqua ions, even if quite unexpected due to notable electrostatic repulsion, has been already revealed in the literature for some other systems. A similar effect was also observed in a bivalent aqueous electrolyte, confined inside carbon micropores under an applied potential.[27] Here, the shortest $M^{2+}\cdots M^{2+}$ distance, evaluated using Extended X-Ray Absorption Fine Structure spectroscopy, was only 2.7 Å, attained by sharing several water molecules between cations. Even more recently a machine-learning potential trained on density functional theory simulations also displayed short $Li^+\cdots Li^+$ distances in a LiCl solution. The state was found to be (strongly) metastable, which is probably due to the much lower concentration of lithium ions (and the absence of nanodomains) compared to the WiS investigated here, but it opens the possibility that such cation pairs are a common feature in concentrated and/or confined aqueous solutions.[28]

In the case of solid-state Li-ion conductors, the most probable $Li^+\cdots Li^+$ distance was reported to be 2.5 Å in an AIMD study of $Li_7La_3Zr_2O_{12}$.[29] Similarly to our system, this short separation of two cations is ensured by charge compensation thanks to several oxygen atoms in the lithium local environment. The only difference is that these oxygen atoms have a fixed position imposed by the crystal structure, while in our case solvent molecules are required to re-arrange in order to stabilize the formed lithium nanochains. From the dynamic point of view, these nanochains are associated to cooperative dynamics and deviations from the Nernst-Einstein approximation for the electrical conductivity.[30,31] Albeit the trajectories provided by AIMD are too short to estimate correctly the diffusion coefficients of the species (let alone the conductivity) as shown in Figure S9a, it is possible to investigate possible correlations by calculating the distinct part of the Van Hove correlation function,[32] which is a time-dependent generalization of the RDF. The $Li^+\cdots Li^+$ function typically displays values larger than 1 at $r = 0$ Å in superionic conductor for times greater than 0 because lithium ions replace each other on the lattice sites of the structure.[31] Despite the liquid character of our system, similar effects are observed in our case as shown on Figure 6, for which correlations begin to be observed at times greater than 20 ps. As a consequence of the strong nanostructuration of the system, dynamic heterogeneities can also be evidenced by calculating the non-gaussian parameter.[33] However, this is not specific to lithium ions only since all the species display heterogeneous dynamics (Figure S9b).

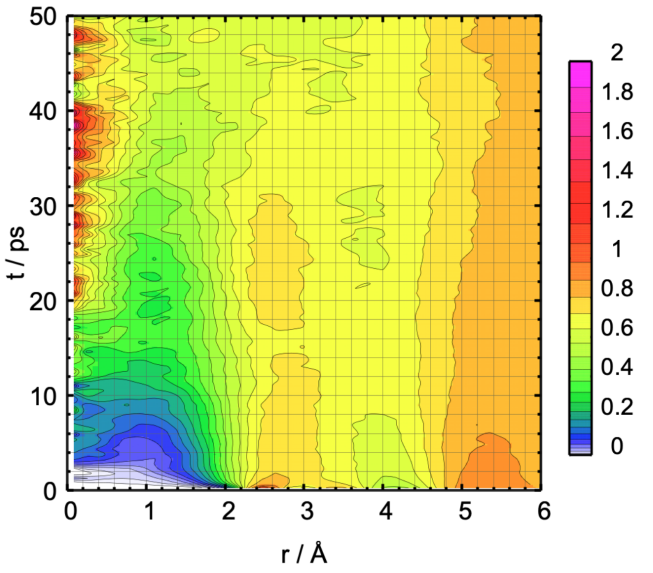

FIG. 6. 3D-plot of the distinct part of the $Li^+\cdots Li^+$ van Hove time-space correlation function. The Li-Li distance (x-axis) is plotted versus the lag time between two trajectory frames (y-axis), and the color scale represents the intensity of the correlation function.

III. CONCLUSIONS

To sum up, we have unveiled an unusual nanochain formation of lithium ions in LiTFSI WiS electrolyte by AIMD simulation. At large distances, the cations have a regular tetrahedral environment, being fully solvated

by water and anion species. On the contrary, at closer distances they arrange into linear nanochains, stabilized by several bridging water molecules, leading to an increase of the lithium coordination number. Due to low free energy barriers, the system remains in dynamic equilibrium, with continuous evolution of the local structure at the nano-scale level. This polymerization-like phenomenon has never been reported before neither by CMD simulations (due to imprecise force fields) nor by earlier AIMD studies (due to small system size). From the dynamic point of view, the Van Hove correlation function raises evidence of a cooperative motion between the lithium ions involved in the chains. In future studies of WiS systems, we encourage to take into account this effect either by reparametrisation of classical force fields or by the use of machine-learning potentials. Future works should track for the existence of similar effects in other ion-concentrated liquids, such as localized high-concentration electrolytes[34,35] or high entropy electrolytes[36–40] that have recently been introduced. High impact of the presence of polymeric species on the interfacial properties is also to be expected, since the concentration of ionic species within the electrochemical double-layer is known to change drastically the local reactivity, such as the formation of dendrites at the metal anodes.

ACKNOWLEDGEMENTS

This work was funded by the European Research Council (ERC) under the European Union Horizon 2020 research and innovation program (grant agreement 771294). Computational tasks were performed using resources provided by EuroHPC Regular Access grant (EHPC-REG-2022R02-244, MeluXina supercomputer, project p200096).

SUPPORTING INFORMATION

The Supporting Information is available free of charge at XXX.

Comparison of the local structure with the literature data, additional simulation snapshots revealing nanochains formation, probability contours revealing the local structure around lithium cations, mean squared displacement, the non-Gaussian parameter, and the simulation results for a small box.

DATA AVAILABILITY STATEMENT

The data (input files and raw data used for the figures) are available on Zenodo at the following address: 10.5281/zenodo.10723288).

METHODS

The studied system was composed of 128 LiTFSI ion pairs and 340 water molecules (3068 atoms in total), corresponding to a molality of 20.9 m. The initial configuration of a periodic cubic box was generated using Packmol.[41] The box length was equal to $l_{x,y,z} = 34.64$ Å, being evaluated from the experimental density.[42]

Prior to the AIMD run, the system was equilibrated by classical MD using LAMMPS.[43] The input files were generated using fftool[44] utility. The Li^+ cation was represented by Aqvist force field,[45] the $TFSI^-$ anion by the CL&P[46] model, and water by SPCE[47] model. The net charge of the ions was scaled by 0.8 in order to accelerate the dynamics. A cutoff of 12 Å was applied for non-bonded interactions, and a tail correction was considered for energy. The particle-particle particle-mash (PPPM) method was used to evaluate electrostatic energies (the accuracy of 10^{-5}). The geometry of water molecules was kept rigid using the SHAKE algorithm. The timestep was set to 1 fs. The system was equilibrated for 20 ns in the NVT ensemble. The Nosé-Hoover thermostat was used to keep the temperature at 298 K.

The AIMD simulation at the Density Functional Theory level was carried out using the QUICKSTEP module[48] of the CP2K package.[49] The last configuration of the classical MD run was used as a starting geometry. The BLYP[50,51] functional plus Grimme D3 correction[52] for van der Waals interactions were adopted, with a combination of Gaussian (DZVP-MOLOPT-SR) plus plane waves basis sets (400 Ry) and GTH pseudopotentials. The nuclei displacements were predicted through classical Newton's equations of motions integrated through the velocity-Verlet algorithm, with a timestep of 0.5 fs. Three-dimensional periodic boundary conditions were applied. The simulation was performed for 70 ps in the NVT ensemble at 298 K, using the Nosé-Hoover thermostat with a constant of 0.1 ps to keep the temperature constant. The equilibrium properties were computed using last 20 ps.

The visualization of the simulation box was done in VMD.[53] The trajectory analysis was performed using TRAVIS[54,55] program and self-written tools. The free energy profile was computed from the corresponding radial distribution function as $F(r) = -k_B T \ln\big(g(r)\big)$.

Additionally, we have performed simulations of a smaller box, containing 64 LiTFSI pairs and 170 H_2O molecules. The obtained results are provided in the Supporting Information (Figure S10).

REFERENCES

[1] T. Liang, R. Hou, Q. Dou, H. Zhang, and X. Yan, "The applications of water-in-salt electrolytes in electrochemical energy storage devices," Adv. Funct. Mater. **31**, 2006749 (2021).
[2] Y. Yamada, K. Usui, K. Sodeyama, S. Ko, Y. Tateyama, and

A. Yamada, "Hydrate-melt electrolytes for high-energy-density aqueous batteries," Nat. Energy **1**, 16129 (2016).
[3]L. Suo, O. Borodin, T. Gao, M. Olguin, J. Ho, X. Fan, C. Luo, C. Wang, and K. Xu, ""Water-in-Salt" Electrolyte Enables High-voltage Aqueous Lithium-ion Chemistries," Science **350**, 938–943 (2015).
[4]M. Amiri and D. Bélanger, "Physicochemical and electrochemical properties of water-in-salt electrolytes," ChemSusChem **14**, 2487–2500 (2021).
[5]O. Borodin, L. Suo, M. Gobet, X. Ren, F. Wang, A. Faraone, J. Peng, M. Olguin, M. Schroeder, M. S. Ding, E. Gobrogge, A. von Wald Cresce, S. Munoz, J. A. Dura, S. Greenbaum, C. Wang, and K. Xu, "Liquid structure with nano-heterogeneity promotes cationic transport in concentrated electrolytes," ACS Nano **11**, 10462–10471 (2017).
[6]J. Vatamanu and O. Borodin, "Ramifications of water-in-salt interfacial structure at charged electrodes for electrolyte electrochemical stability," J. Phys. Chem. Lett. **8**, 4362–4367 (2017).
[7]J. Zheng, G. Tan, P. Shan, T. Liu, J. Hu, Y. Feng, L. Yang, M. Zhang, Z. Chen, Y. Lin, J. Lu, J. C. Neuefeind, Y. Ren, K. Amine, L.-W. Wang, K. Xu, and F. Pan, "Understanding thermodynamic and kinetic contributions in expanding the stability window of aqueous electrolytes," Chem **4**, 2872–2882 (2018).
[8]R. Bouchal, Z. Li, C. Bongu, S. Le Vot, R. Berthelot, B. Rotenberg, F. Favier, S. A. Freunberger, M. Salanne, and O. Fontaine, "Competitive salt precipitation/dissolution during free-water reduction in water-in-salt electrolyte," Angew. Chem., Int. Ed. **132**, 16047–16051 (2020).
[9]Y. Zhang, N. H. C. Lewis, J. Mars, G. Wan, N. J. Weadock, C. J. Takacs, M. R. Lukatskaya, H.-G. Steinrück, M. F. Toney, A. Tokmakoff, and E. J. Maginn, "Water-in-Salt LiTFSI aqueous electrolytes. 1. Liquid structure from combined molecular dynamics simulation and experimental studies," J. Phys. Chem. B **125**, 4501–4513 (2021).
[10]Y. Zhang and E. J. Maginn, "Water-In-Salt LiTFSI aqueous electrolytes (2): Transport properties and Li^+ dynamics based on molecular dynamics simulations," J. Phys. Chem. B **125**, 13246–13254 (2021).
[11]A. Tot and L. Kloo, "Water-in-salt electrolytes –molecular insights to the high solubility of lithium-ion salts," Chem. Commun. **58**, 9528–9531 (2022).
[12]J. Jeon, H. Lee, J.-H. Choi, and M. Cho, "Modeling and simulation of concentrated aqueous solutions of LiTFSI for battery applications," J. Phys. Chem. C **124**, 11790–11799 (2020).
[13]D. Reber, N. Takenaka, R.-S. Kühnel, A. Yamada, and C. Battaglia, "Impact of anion asymmetry on local structure and supercooling behavior of water-in-salt electrolytes," J. Phys. Chem. Lett. **11**, 4720–4725 (2020).
[14]T. Mendez-Morales, Z. Li, and M. Salanne, "Computational screening of the physical properties of water-in-salt electrolytes," Batter. Supercaps **4**, 646–652 (2021).
[15]Z. Yu, L. A. Curtiss, R. E. Winans, Y. Zhang, T. Li, and L. Cheng, "Asymmetric composition of ionic aggregates and the origin of high correlated transference number in water-in-salt electrolytes," J. Phys. Chem. Lett. **11**, 1276–1281 (2020).
[16]M. A. González, O. Borodin, M. Kofu, K. Shibata, T. Yamada, O. Yamamuro, K. Xu, D. L. Price, and M.-L. Saboungi, "Nanoscale relaxation in "water-in-salt"and "water-in-bisalt" electrolytes," J. Phys. Chem. Lett. **11**, 7279–7284 (2020).
[17]M. A. González, H. Akiba, O. Borodin, G. J. Cuello, L. Hennet, S. Kohara, E. J. Maginn, L. Mangin-Thro, O. Yamamuro, Y. Zhang, D. L. Price, and M.-L. Saboungi, "Structure of water-in-salt and water-in-bisalt electrolytes," Phys. Chem. Chem. Phys. **24**, 10727–10736 (2022).
[18]S. Perez Beltran, X. Cao, J.-G. Zhang, and P. Balbuena, "Localized high concentration electrolytes for high voltage lithium–metal batteries: Correlation between the electrolyte composition and its reductive/oxidative stability," Chem. Mater. **32**, 5973–5984 (2020).
[19]S. Perez Beltran, X. Cao, J.-G. Zhang, P. Z. El-Khoury, and P. B. Balbuena, "Influence of diluent concentration in localized high concentration electrolytes: elucidation of hidden diluent-li^+ interactions and li^+ transport mechanism," J. Mater. Chem. A **9**, 17459–17473 (2021).
[20]T. Malaspina, G. Colherinhas, S. E. Weitzner, B. C. Wood, and E. Eterno Fileti, "Unraveling local structures of salt-in-water and water-in-salt electrolytes via ab initio molecular dynamics," J. Mol. Liq. **383**, 122097 (2023).
[21]K. Miyazaki, N. Takenaka, E. Watanabe, S. Iizuka, Y. Yamada, Y. Tateyama, and A. Yamada, "First-principles study on the peculiar water environment in a hydrate-melt electrolyte," J. Phys. Chem. Lett. **10**, 6301–6305 (2019).
[22]F. Wang, Y. Sun, and J. Cheng, "Switching of redox levels leads to high reductive stability in water-in-salt electrolytes," J. Am. Chem. Soc. **145**, 4056–4064 (2023).
[23]A. Serva, N. Dubouis, A. Grimaud, and M. Salanne, "Confining water in ionic and organic solvents to tune its adsorption and reactivity at electrified interfaces," Acc. Chem. Res. **54**, 1034–1042 (2021).
[24]Z. Li, *"Water-in-salt" electrolyte for supercapacitors: a molecular dynamics study*, Ph.D. thesis, Sorbonne University (2018).
[25]A. Triolo, V. Di Lisio, F. Lo Celso, G. B. Appetecchi, B. Fazio, P. Chater, A. Martinelli, F. Sciubba, and O. Russina, "Liquid structure of a water-in-salt electrolyte with a remarkably asymmetric anion," J. Phys. Chem. B **125**, 12500–12517 (2021).
[26]J. DiStasio, Robert A., B. Santra, Z. Li, X. Wu, and R. Car, "The individual and collective effects of exact exchange and dispersion interactions on the ab initio structure of liquid water," The Journal of Chemical Physics **141**, 084502 (2014).
[27]J. Wei, L. Zhong, H. Xia, Z. Lv, C. Diao, W. Zhang, X. Li, Y. Du, S. Xi, M. Salanne, X. Chen, and S. Li, "Metal-ion oligomerization inside electrified carbon micropores and its effect on capacitive charge storage," Adv. Mater **34**, 2107439 (2022).
[28]J. Zhang, J. Pagotto, T. Gould, and T. T. Duignan, "Accurate, fast and generalisable first principles simulation of aqueous lithium chloride," (2023), arXiv:2310.12535 [physics.chem-ph].
[29]K. Meier, T. Laino, and A. Curioni, "Solid-state electrolytes: Revealing the mechanisms of li-ion conduction in tetragonal and cubic llzo by first-principles calculations," J. Phys. Chem. C **118**, 6668–6679 (2014).
[30]M. Burbano, D. Carlier, F. Boucher, B. J. Morgan, and M. Salanne, "Sparse cyclic excitations explain the low ionic conductivity of stoichiometric $li_7la_3zr_2o_{12}$," Phys. Rev. Lett. **116**, 135901 (2016).
[31]X. He, Y. Zhu, and Y. Mo, "Origin of fast ion diffusion in superionic conductors," Nat. Commun. **8**, 15893 (2017).
[32]L. Van Hove, "Correlations in space and time and born approximation scattering in systems of interacting particles," Phys. Rev. **95**, 249–262 (1954).
[33]F. Chen and M. Forsyth, "Elucidation of transport mechanism and enhanced alkali ion transference numbers in mixed alkali metal–organic ionic molten salts," Phys. Chem. Chem. Phys. **18**, 19336–19344 (2016).
[34]S. Chen, J. Zheng, D. Mei, K. S. Han, M. H. Engelhard, W. Zhao, W. Xu, J. Liu, and J.-G. Zhang, "High-voltage lithium-metal batteries enabled by localized high-concentration electrolytes," Adv. Mat. **30**, 1706102 (2018).
[35]J.-G. Zhang, W. Xu, J. Xiao, X. Cao, and J. Liu, "Lithium metal anodes with nonaqueous electrolytes," Chem. Rev. **120**, 13312–13348 (2020).
[36]S. C. Kim, J. Wang, R. Xu, P. Zhang, Y. Chen, Z. Huang, Y. Yang, Z. Yu, S. T. Oyakhire, W. Zhang, L. C. Greenburg, M. S. Kim, D. T. Boyle, P. Sayavong, Y. Ye, J. Qin, Z. Bao, and C. Yi, "High-entropy electrolytes for practical lithium metal batteries," Nat. Energy **8**, 814–826 (2023).
[37]C. Yang, J. Xia, C. Cui, T. P. Pollard, J. Vatamanu, A. Faraone, J. A. Dura, M. Tyagi, A. Kattan, E. Thimsen, J. Xu, W. Song, E. Hu, X. Ji, S. Hou, X. Zhang, M. S. Ding, S. Hwang, D. Su, Y. Ren, X.-Q. Yang, H. Wang, O. Borodin, and C. Wang, "All-temperature zinc batteries with high-entropy aqueous elec-

trolyte," Nat. Sustain. **6**, 325–335 (2023).
[38]Q. Wang, C. Zhao, J. Wang, Z. Yao, S. Wang, S. G. H. Kumar, S. Ganapathy, S. Eustace, X. Bai, B. Li, and M. Wagemaker, "High entropy liquid electrolytes for lithium batteries," Nat. Commun. **14**, 440 (2023).
[39]Q. Wang, C. Zhao, Z. Yao, J. Wang, F. Wu, S. G. H. Kumar, S. Ganapathy, S. Eustace, X. Bai, B. Li, J. Lu, and M. Wagemaker, "Entropy-driven liquid electrolytes for lithium batteries," Adv. Mater. **35**, 2210677 (2023).
[40]H. Ji, C. Xie, T. Wu, H. Wang, Z. Cai, Q. Zhang, W. Li, L. Fu, H. Li, and H. Wang, "High-entropy solvent design enabling a universal electrolyte with a low freezing point for low-temperature aqueous batteries," Chem. Commun. **59**, 8715–8718 (2023).
[41]L. Martínez, R. Andrade, E. G. Birgin, and J. M. Martínez, "PACKMOL: A package for building initial configurations for molecular dynamics simulations," J. Comp. Chem. **30**, 2157–2164 (2009).
[42]W. J. R. Gilbert, J. Safarov, D. L. Minnick, M. A. Rocha, E. P. Hassel, and M. B. Shiflett, "Density, viscosity, and vapor pressure measurements of water + lithium bis(trifluoromethylsulfonyl)imide solutions," J. Chem. Eng. Data **62**, 2056–2066 (2017).
[43]A. P. Thompson, H. M. Aktulga, R. Berger, D. S. Bolintineanu, W. M. Brown, P. S. Crozier, P. J. in 't Veld, A. Kohlmeyer, S. G. Moore, T. D. Nguyen, R. Shan, M. J. Stevens, J. Tranchida, C. Trott, and S. J. Plimpton, "Lammps - a flexible simulation tool for particle-based materials modeling at the atomic, meso, and continuum scales," Computer Physics Communications **271**, 108171 (2022).
[44]A. A. H. Padua, "github.com/paduagroup/fftool," (2022), (accessed 2 December 2022).
[45]J. Åqvist, "Ion-water interaction potentials derived from free energy perturbation simulations," J. Phys. Chem. **94**, 8021–8024 (1990).
[46]J. N. Canongia Lopes, J. Deschamps, and A. A. H. Pádua, "Modeling Ionic Liquids Using a Systematic All-Atom Force Field," J. Phys. Chem. B **108**, 2038–2047 (2004).
[47]H. J. C. Berendsen, J. R. Grigera, and T. P. Straatsma, "The missing term in effective pair potentials," J. Phys. Chem. **91**, 6269–6271 (1987).
[48]J. VandeVondele, M. Krack, F. Mohamed, M. Parrinello, T. Chassaing, and J. Hutter, "Quickstep: Fast and accurate density functional calculations using a mixed gaussian and plane waves approach," Comput. Phys. Commun. **167**, 103–128 (2005).
[49]J. Hutter, M. Iannuzzi, F. Schiffmann, and J. VandeVondele, "cp2k: atomistic simulations of condensed matter systems," Wiley Interdiscip. Rev. Comput. Mol. **4**, 15–25 (2014).
[50]A. D. Becke, "Density-functional exchange-energy approximation with correct asymptotic behavior," Phys. Rev. A **38**, 3098–3100 (1988).
[51]C. Lee, W. Yang, and R. G. Parr, "Development of the Colle-Salvetti correlation-energy formula into a functional of the electron density," Phys. Rev. B **37**, 785–789 (1988).
[52]S. Grimme, J. Antony, S. Ehrlich, and H. Krieg, "A consistent and accurate ab initio parametrization of density functional dispersion correction (DFT-D) for the 94 elements H-Pu," J. Chem. Phys. **132**, 154104 (2010).
[53]W. Humphrey, A. Dalke, and K. Schulten, "VMD: Visual molecular dynamics," J. Mol. Graph. **14**, 33–38 (1996).
[54]M. Brehm and B. Kirchner, "TRAVIS - a free analyzer and visualizer for Monte Carlo and molecular dynamics trajectories," J. Chem. Inf. Model. **51**, 2007–2023 (2011).
[55]M. Brehm, M. Thomas, S. Gehrke, and B. Kirchner, "TRAVIS—a free analyzer for trajectories from molecular simulation," J. Chem. Phys. **152**, 164105 (2020).

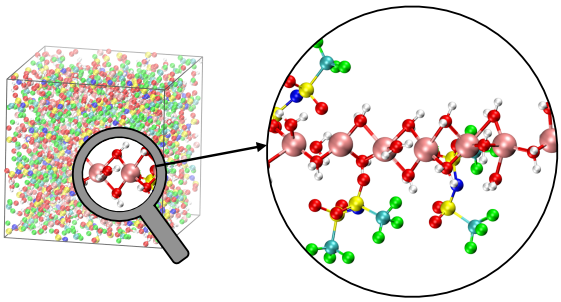

FIG. 7. TOC Graphic